SAND2021-6264 PE
SAND2020-6511 PE

CENTER FOR COMPUTING RESEARCH

Sandia National Laboratories

Data-driven, compact models for radiation-induced photocurrent effects

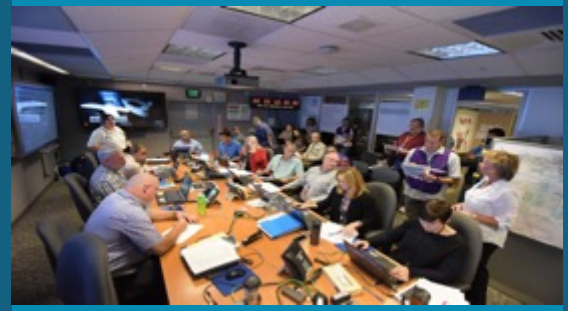


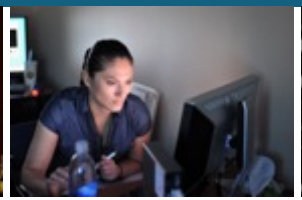
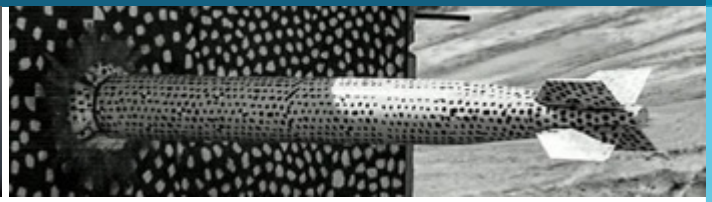

Irish Numerical Analysis Forum seminar

April 7, 2022

PRESENTED BY

Pavel Bochev

Collaborators: J. Hanson, C. Hembree, E.Keiter, B. Paskaleva, P. Kuberry

LDRD LABORATORY DIRECTED RESEARCH & DEVELOPMENT

U.S. DEPARTMENT OF ENERGY | Office of Science

ASCR

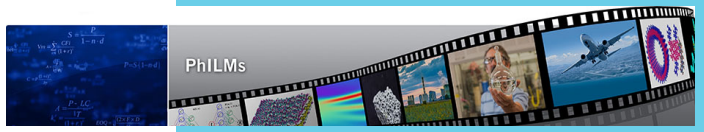

U.S. DEPARTMENT OF ENERGY NNSA

Sandia National Laboratories is a multimission laboratory managed and operated by National Technology & Engineering Solutions of Sandia, LLC, a wholly owned subsidiary of Honeywell International Inc., for the U.S. Department of Energy's National Nuclear Security Administration under contract DE-NA0003525.

Radiation-induced photocurrents

What is it?

- Fluence of ionizing radiation generates **excess electron-hole pairs** within a semiconductor device
- Resulting **excess current** is not present in normal environments and **alters device characteristics**
- This can lead to **abnormal circuit behavior** and operation (does not function as intended)

Why it matters

Radiation induced photocurrents are a major concern for electronic applications requiring a **high level of reliability**:

- **Nuclear weapons:** hostile environments can compromise weapon's circuits such as AFF
- **Space electronics:** trapped radiation, solar activity, galactic cosmic rays pose significant risks to navigation and communication satellites
- **Medical electronics:** high energy ionizing particles and photons are used extensively for medical diagnostics and treatment

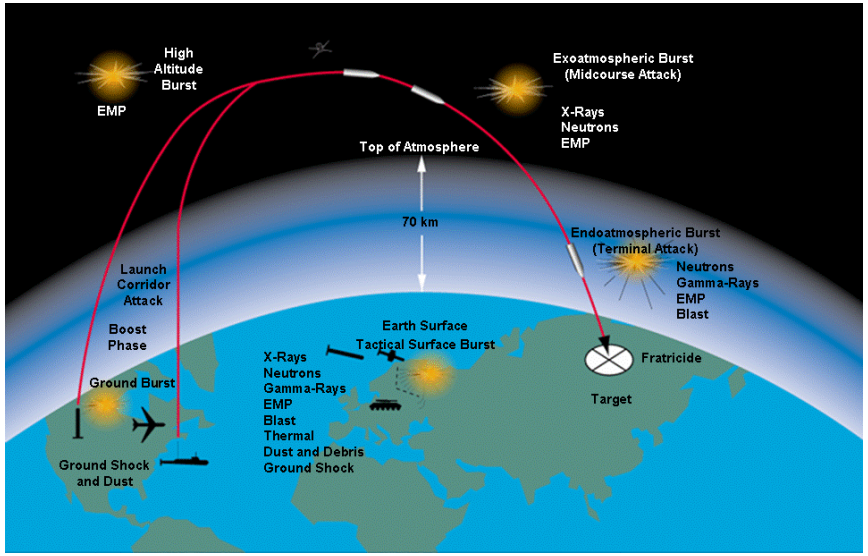

S. Meyers, QASPR Overview, 2007; E. Bielejec, SAND2007-0364

Mitigation

Development of a range of hardness assurance methodologies & rad hardened devices

Modeling and simulation plays a key role in understanding and mitigating radiation effects

Modeling and simulation of photocurrent effects

Option #1: TCAD (Technology Computer-Aided Design)

- First-principles semiconductor device models provide accurate descriptions of device physics over a wide range of operating conditions
- However, TCAD simulations are computationally expensive and almost never used in circuit simulators (so-called mixed mode simulations)

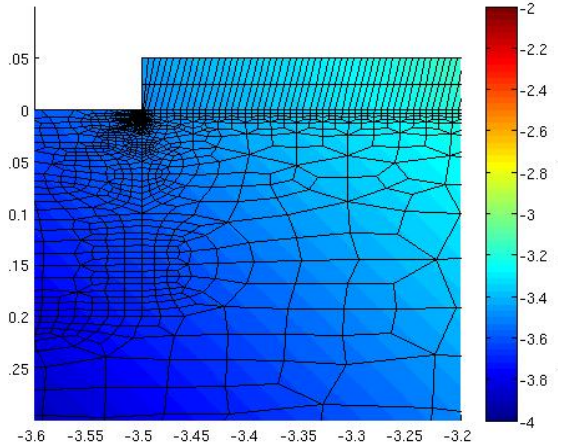

CHARON MOSFET simulation

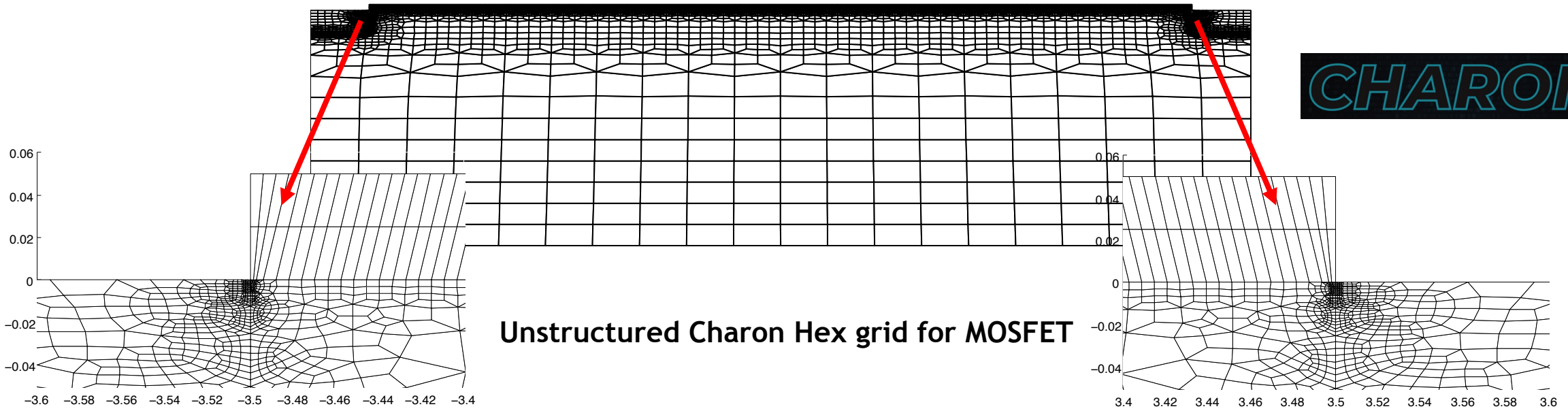

Unstructured Charon Hex grid for MOSFET

Compact device models

Option #2: Compact Device Models

- **Computationally inexpensive**: combination of
  - empirical formulas for ideal circuit elements
  - simplified solutions to semiconductor transport equations
  - circuit models combining the above

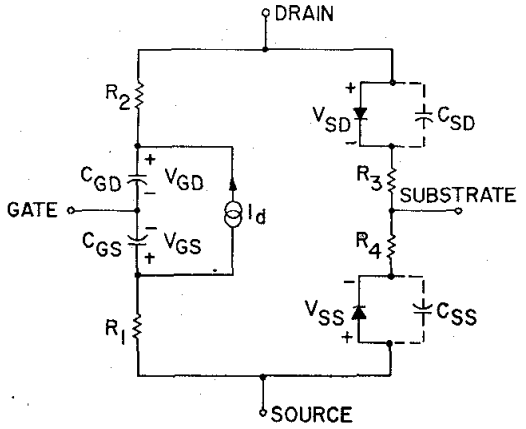

Shockley diode equation

$$I = I_s\left(\exp\left(\frac{V_D}{nV_T}\right) - 1\right)$$

p-channel IGFET circuit model. Shichman et al, IEEE Journal of Solid-State Circuits, 3(3):285–289, 1968.

Sandia has led/sponsored the development of most compact photocurrent models currently in use.

Dominant approach (50+ years): based on analytic solutions of the governing PDEs.

- Analytic solutions require empirical assumptions with limited validity to render the PDEs solvable in closed form.
- Reliance on simplified solutions compromises ability of the models to generalize.
- Models may have to be recalibrated for different operating regimes.
- Models can not take advantage of the full-featured physics deployed in TCAD.

Despite the successes of data-driven and reduced order models in other science and engineering fields they have not yet been embraced by the radiation effects community

Ongoing projects at Sandia aim to “disrupt” this status quo by demonstrating that **numerical data-driven approaches** are a viable alternative to analytic approximations.

Development of traditional compact photocurrent models

Compact analytic photocurrent models are developed by treating separately different device regions

- This is required to render the Drift-Diffusion equations solvable in closed form

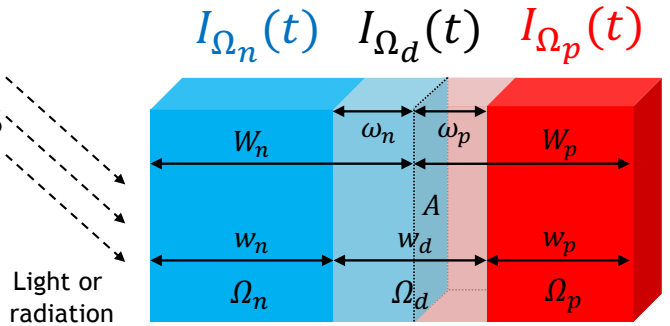

Step 1: Split device into a depletion region and quasi-neutral *P* and *N*-regions

Carriers in Ω_d are quickly converted to *prompt photocurrent* (strong electric field)

Carriers in Ω_p, Ω_n gradually drift and/or diffuse into Ω_d: produce *delayed photocurrents*

Step 2: Total photocurrent is sum of independent contributions: $I(t) = I_{\Omega_p}(t) + I_{\Omega_n}(t) + I_{\Omega_d}(t)$

Model $I_{\Omega_d}(t)$ using the depletion approximation: Drift-Diffusion ⇢ Poisson Equation ⇢ $I_{\Omega_d}(t) = qgAw_d$

Model $I_{\Omega_p}(t)$ and $I_{\Omega_n}(t)$ using charge neutrality + congruence + low injection rate assumptions

Drift-Diffusion ⇢ Ambipolar Diffusion Equation (ADE) in Ω_n:

$$\frac{\partial \delta p}{\partial t} = D_p \frac{\partial^2 \delta p}{\partial x^2} - \mu_p E_n \frac{\partial \delta p}{\partial x} - \frac{\delta p}{\tau_p} + g(x,t), \quad (x,t) \in \Omega_n \times T$$

Photocurrent generated in Ω_n (homogeneous BC)

$$I_{\Omega_n}(t) = qAD_p \frac{\partial \delta p}{\partial x}(w_n, t) + \cancel{\mu E_n \delta p(w_n, t)}$$

Development of traditional compact photocurrent models

Step 3: Further simplify ADE so that one solve it analytically

Wirth & Rogers Model, IEEE Trans. Nucl. Sci. 11 (1964):

- Unbounded N and P regions
- Negligible electric field: $E = 0$ (no drift term)

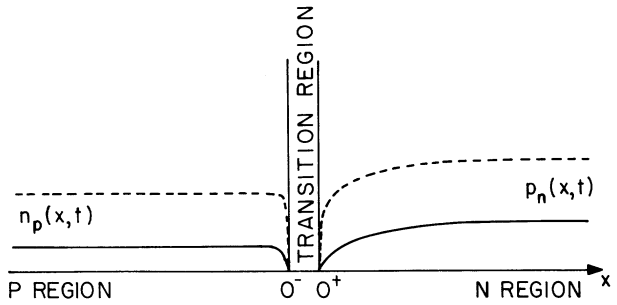

Enlow & Alexander Model, IEEE Trans. Nucl. Sci. 35 (1988):

- Use approximate Laplace transforms: inaccurate if $E>10V/cm$

Fjeldly at al Model, IEEE Trans. Nucl. Sci. 48 (2001):

- "Separation of variables" form

$$I^N_{delay} = g(t)L_p \tanh\left(\frac{W_p}{2L_p}\right)$$

Implemented in Xyce

Wunsch, Axness & Kerr Model, J. Appl. Phys. 96 (2004):

- Use Fourier analysis techniques:

$$I^N_{delay} = 4q\frac{L_p^2}{x_1}\sum_{m=0}^{\infty}\int_0^{t/\tau_p} g(t-u\tau_p)e^{-a_m u}du$$

Development of traditional compact photocurrent models

Step 4: Use lab measurements to calibrate the compact model

ion beam lab

Ion Beams

- **Microbeams:** typically $< 1\mu m$ in diameter, but very low ion currents typically 1000 to 10,000 ions/s
- **Milli-beams:** (typical QASPR beams) ~ $200\times200\mu m^2$ to $4\times5mm^2$, high ion flux achieving $> 3\times10^{18}\ n/cm^2/s\ MeV(Si)$, the spot size is continuously variable over these ranges.

Electron Beams

- **Milli-beams:** ~ $200\times200\mu m^2$ to $4\times4mm^2$, but only able to achieve the highest dose rates $> 1\times10^{12}\ rad(Si)/s$ over ~ $1\times1mm^2$ (limited by beam current)

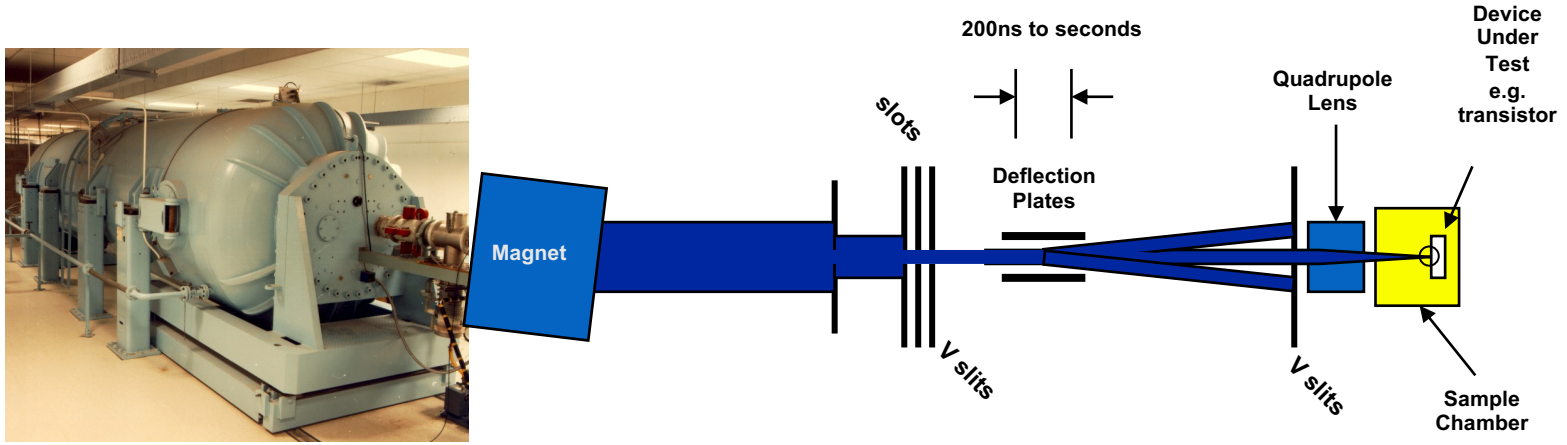

http://www.sandia.gov/pcnsc/research/research-briefs/briefs-2007.html

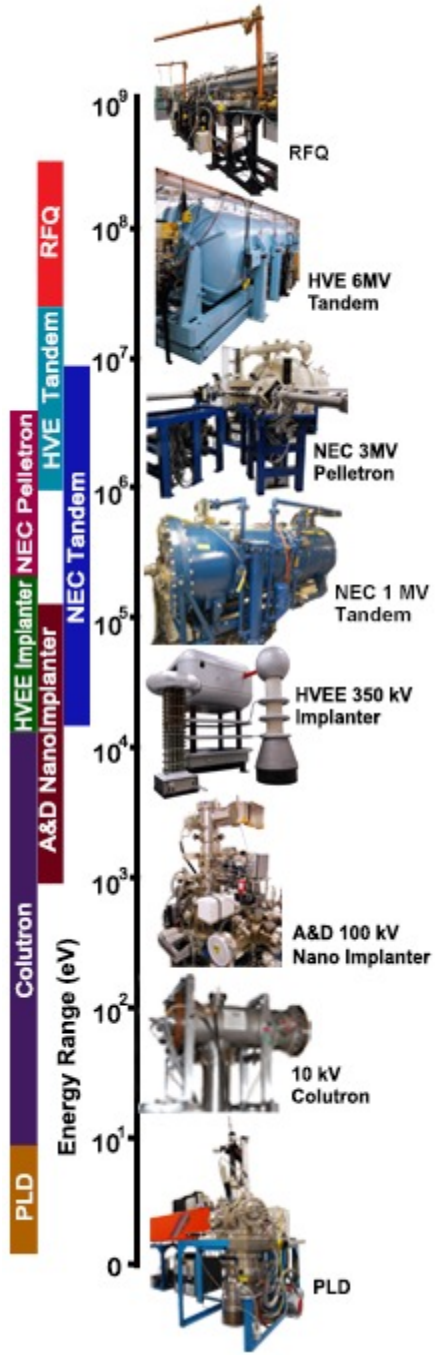

Figure credit: Edward Bielejec, SNL

Hybrid compact models

Recall that:

- Closed form solutions require empirical assumptions with limited validity
- Reliance on simplified solutions compromises ability of the models to generalize.
- Models may have to be recalibrated for different operating regimes

Hybrid compact models: a first step towards building trust in alternative, numerical approaches

- Retain the separate treatment of the depletion and quasi-neutral regions
- Focus on the delay photocurrent as it is the more challenging aspect of the model development
- Replace the analytic solution by a data-driven numerical model, thus a **hybrid** analytic-numerical approach.

We have developed three types of hybrid models differing in their "physics-informed (PI)" levels:

- Dynamic Mode Decomposition model: **minimal PI** - generic model form, learns entirely from data
- A data-driven exponential time integrator: **moderate PI** - model form informed by ADE,
- Projection-based reduced order model (ROM): **maximum PI** - compact model derived from the ADE

All models are discrete or continuous time dynamical systems with inputs, simulating the internal state of the device:

$$\boldsymbol{x}_{k+1} = \mathbf{A}\boldsymbol{x}_k + \mathbf{B}\boldsymbol{g}_k \qquad \dot{x}(t) = \mathbf{A}x(t) + \mathbf{B}g(t)$$

P. Bochev and B. Paskaleva. Development of data-driven exponential integrators with application to modeling of delay photocurrents. *Num. Meth. PDE,* 2021.

J. Hanson, P. Bochev, and B. Paskaleva. Learning compact physics-aware delayed photocurrent models using DMD. *The ASA Data Science Journal*, 2020.

J. Hanson, B. Paskaleva, E. Keiter, P. Bochev, and C. Hembree. A hybrid analytic-numerical compact model for radiation induced photocurrent effects. IEEE Transactions on Nuclear Science, 69(2):160–168, 2022.

Dynamic Mode Decomposition model

J. Hanson et al. Learning compact physics-aware delayed photocurrent models using dynamic mode decomposition. *Statistical Analysis and Data Mining: The ASA Data Science Journal*, 2020.

System identification step

Collect samples: $X = \begin{bmatrix} | & & | \\ \mathbf{u}_0 & \cdots & \mathbf{u}_{m-1} \\ | & & | \end{bmatrix}$; $X' = \begin{bmatrix} | & & | \\ \mathbf{u}_1 & \cdots & \mathbf{u}_{m} \\ | & & | \end{bmatrix}$; and $G = \begin{bmatrix} | & & | \\ \mathbf{g}_0 & \cdots & \mathbf{g}_{m-1} \\ | & & | \end{bmatrix}$

Arrange samples: $X' = AX + BG = \begin{bmatrix} A & B \end{bmatrix} \begin{bmatrix} X \\ G \end{bmatrix} =: \begin{bmatrix} A & B \end{bmatrix} S$

DMD with control inputs

Solve for *A* and *B*: $\begin{bmatrix} A & B \end{bmatrix} \approx \begin{bmatrix} \bar{A} & \bar{B} \end{bmatrix} := X' S^{\dagger}$

Order Reduction step

Truncate the SVD for *S* (# modes to identify): $S^{\dagger} = \tilde{V}\tilde{\Sigma}^{-1}\tilde{U}^{\mathsf{T}}$

$$A \approx \bar{A} \approx X'\tilde{V}\tilde{\Sigma}^{-1}\tilde{U}_1{}' \in \mathbb{R}^{n\times n}$$
$$B \approx \bar{B} \approx X'\tilde{V}\tilde{\Sigma}^{-1}\tilde{U}_2{}^{\mathsf{T}} \in \mathbb{R}^{n\times n}$$

Truncate the SVD for *X'* (# modes to model): $X' \approx \hat{U}\hat{\Sigma}\hat{V}^{\mathsf{T}}$

$$\tilde{A} := \hat{U}^{\mathsf{T}}\bar{A}\hat{U} = \hat{U}^{\mathsf{T}}X'\tilde{V}\tilde{\Sigma}^{-1}\tilde{U}_1{}^{\mathsf{T}}\hat{U} \in \mathbb{R}^{r\times r}$$
$$\tilde{B} := \hat{U}^{\mathsf{T}}\bar{B} \quad = \hat{U}^{\mathsf{T}}X'\tilde{V}\tilde{\Sigma}^{-1}\tilde{U}_2{}^{\mathsf{T}} \in \mathbb{R}^{r\times n}$$

Final Model:

$$\tilde{\mathbf{u}}_{k+1} = \tilde{A}\tilde{\mathbf{u}}_k + \tilde{B}\mathbf{g}_k$$
$$\tilde{\mathbf{u}}_0 = \hat{U}^{\mathsf{T}}\mathbf{u}_0$$
$$\mathbf{u}_k \approx \hat{U}\tilde{\mathbf{u}}_k,$$

A data-driven exponential time integrator

A data-driven exponential time integrator

Bochev et al. Development of data-driven exponential integrators with application to modeling of delay photocurrents. *Num. Meth. PDEs., 2021*

Discretized ADE: $\dot{u}(t) = Qu(t) + g(t)$ ➡ $u^{n+1} \approx \exp(\Delta t Q)u^n + g^n \int_{t^n}^{t^{n+1}} \exp(Qt^{n+1} - \tau)d\tau$

$$\boldsymbol{u}^{n+1} := A\boldsymbol{u}^n + B\boldsymbol{g}^n \qquad A := (I + \Delta t \Phi Q) \qquad B := \Delta t \Phi$$

➡

$$\Phi(\Delta t Q) = \frac{1}{\Delta t} Q^{-1}(\exp(\Delta t Q) - I)$$ ETI dynamic term

$$Q = \mathcal{L}_{ADE}^h$$ ETI spatial term

Learning strategy & properties:

- **Spatial term:** operator regression based on a weak Galerkin form
- **Dynamic term:** a DMD-like approach that works on pulse rather than time series
- It is possible to learn Φ and Q independently if u^n=0 (usually true)
- Good stability properties, requires less data than DMD

Projection-based ROM

J. Hanson, B. Paskaleva, E. Keiter, P. Bochev, and C. Hembree. A hybrid analytic-numerical compact model for radiation induced photocurrent effects. IEEE Transactions on Nuclear Science, 69(2):160–168, 2022.

Discretize the ADE in 1D using finite elements: $\frac{\partial \delta p}{\partial t} = D_p \frac{\partial^2 \delta p}{\partial x^2} - \mu_p E_n \frac{\partial \delta p}{\partial x} - \frac{\delta p}{\tau_p} + g(x,t), \qquad (x,t) \in \Omega_n \times T$

Full-Order Model (FOM):

$$\dot{\boldsymbol{u}}(t) = (A + E(t)B)\boldsymbol{u}(t) + \boldsymbol{g}(t)$$
$$\boldsymbol{u}(t) \coloneqq \left(u_1(t), \cdots, u_{m-1}(t)\right) \in \mathbb{R}^{m-1} \qquad u_{\mathrm{ADE}}(x,t) = \sum_{i=1}^{m-1} u_i(t) v_i(x)$$

- $\frac{\partial \delta p}{\partial x}(w_n, t)$ in the boundary current computed via gradient of shape functions: $\frac{\partial \delta p}{\partial x}(w_n, t) \leftarrow \sum_{i=1}^{m-1} u_i(t) \frac{dv_i}{dx}(w_n)$
- Find a change of coordinates so that only a few of u_i's in the FOM are "active" and most are near zero.
- We wish to project the high-dimensional state $\boldsymbol{u} \in \mathbb{R}^{m-1}$ onto a low-dimensional hyperplane: $\tilde{\boldsymbol{u}} \coloneqq P\boldsymbol{u} \in \mathbb{R}^r$
- With *P* determined, we can compute the pushforward dynamics for $\tilde{\boldsymbol{u}}$ (*r*-dimensional system of ODEs).

Projection-based ROM

- How do we identify *P*? Truncated SVD:

$$X = \begin{bmatrix} | & & | \\ \boldsymbol{u}_1 & \cdots & \boldsymbol{u}_q \\ | & & | \end{bmatrix} = [\tilde{U} \quad \tilde{U}_{\text{trun}}] \begin{bmatrix} \tilde{\Sigma}^T & 0 \\ 0 & \tilde{\Sigma}_{\text{trun}}^T \end{bmatrix} \begin{bmatrix} \tilde{V}^T \\ \tilde{V}_{\text{trun}}^T \end{bmatrix} \approx \tilde{U}\tilde{\Sigma}\tilde{V}^T$$

where $0 < r \leq m - 1$ modes are preserved, and $m - 1 - r$ modes are truncated.

- Now $P = \tilde{U}^T$ and the *reduced-order model* (ROM) is a system of r ODEs

$$\dot{\tilde{\boldsymbol{u}}}(t) = \left(\tilde{A} + \boldsymbol{E}(t)\tilde{B}\right)\tilde{\boldsymbol{u}}(t) + \tilde{U}^T\boldsymbol{g}(t)$$
$$\tilde{\boldsymbol{u}}(0) = \tilde{U}^T\boldsymbol{u}(0)$$
$$\boldsymbol{u}(t) \approx \tilde{U}\tilde{\boldsymbol{u}}(t)$$

where $\tilde{A} = \tilde{U}^T A\tilde{U} \in \mathbb{R}^{r\times r}$ and $\tilde{B} = \tilde{U}^T B\tilde{U} \in \mathbb{R}^{r\times r}$

For an effective ROM we want: $r \ll m - 1$

Verification: synthetic device test

We apply the DMD and ETI models to solve a radiation pulse test problem for a synthetic device described in C. L. Axness, B. Kerr, T. F. Wunsch. J. Appl. Phys., 2004

Setting up the device: lightly doped diode

- $D_p = 1.19\times10^{1} cm^2/s$ - diffusion
- $\mu_p = 4.64\times10^{2} cm^2/Vs$ - carrier mobility
- $L_p = 1.54\times10^{-2} cm^2/s$ - diffusion length
- $\tau_p = 1.97\times10^{-5} s$ - carrier lifetime
- $E = -20V/cm$ or $E = 0$ - electric field

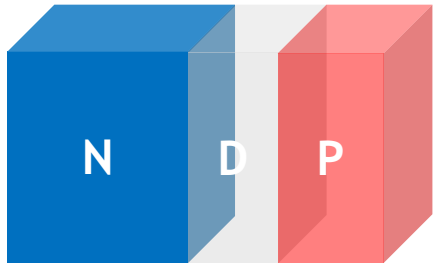

Dimensions representative of discrete devices such as

- Zener voltage regulator,
- 1N6625 ultrafast rectifier,
- 1N4148 switching diode

- $x_N = 2L_p = 3.08\times10^{-2} cm$ - length of the N-region
- $C = 10^{17} cm^2$ - doping concentration

Generation rate (source term):

- $1.0\mu s$ step pulse, constant over the N-region: models irradiation of the entire device
- Dose rate $\gamma = 10^{9} rad(Si)/s$
- Generation density $= 4.3\times10^{22}\ cm^{-3}/s$.

In all cases we run the simulation until $t_{final} = 5\mu s$.

Synthetic device data used in the model development

"The response most useful in experimental studies is that caused by a short pulse of radiation[1]."

(Otherwise you may cause irreversible damage or even destroy your device) 

- Our synthetic data will simulate device scans by N^b **electron beams** with
  - $R = 100{\sim}500\mu m$, duration $T = 0.1{\sim}0.5\mu s$, and dose rate $\gamma = 10^9 rad(Si)/s$
- "Experimental" data set obtained by solving ADE on a very fine mesh in the **N-region**
- ADE parameters set to correspond to a lightly doped diode:

$$D_p = 1.19{\times}10^1 cm^2/s \qquad x_N = 2L_p = 3.08{\times}10^{-2} cm$$
$$L_p = 1.54{\times}10^{-2} cm^2/s \qquad E = -20V/cm \text{ or } E = 0$$
$$\tau_p = 1.97{\times}10^{-5} s \qquad C = 10^{17} cm^2$$

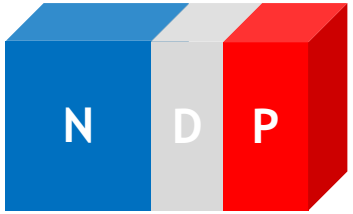

$$G^k = \begin{bmatrix} \vdots & \cdots & \vdots \\ \boldsymbol{g}_1^k & \ddots & \boldsymbol{g}_{N^b}^k \\ \vdots & \cdots & \vdots \end{bmatrix};\ X^k = \begin{bmatrix} \vdots & \cdots & \vdots \\ \boldsymbol{u}_1^k & \ddots & \boldsymbol{u}_{N^b}^k \\ \vdots & \cdots & \vdots \end{bmatrix};\ \boldsymbol{g}_i^k, \boldsymbol{u}_i^k \in \boldsymbol{R}^{N^n}$$

$k = 0,1,\ldots,N^T$

N^T - time series length

N^n - number of nodes

- **Training data sets for the model obtained by down-sampling this "experimental" data.**

Typical "experimental" data

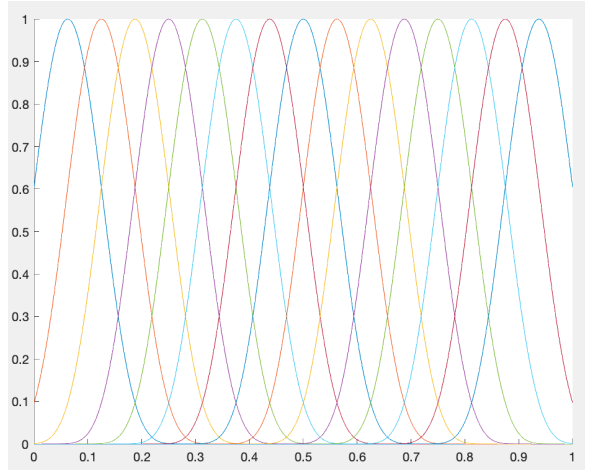

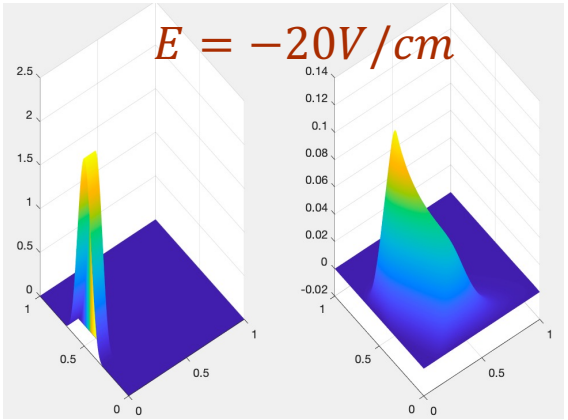

[1]Wirth & Rogers, IEEE Trans. Nucl. Sci. 11 (1964)

Verification: DMD, ETI delayed photocurrent models for a synthetic device

- We use the models to estimate the delayed photocurrent contributed by the quasi-neutral *N* region Ω_n of a lightly doped diode irradiated by $1.0\mu s,\ 10^9 rad(Si)/s$ step pulse.
- We compare to published results by Axness et al. JAP, 2004 for the case $x_N = 2L_p$ ($\xi_p = 2$ in the figure).

$E = -20V/cm$

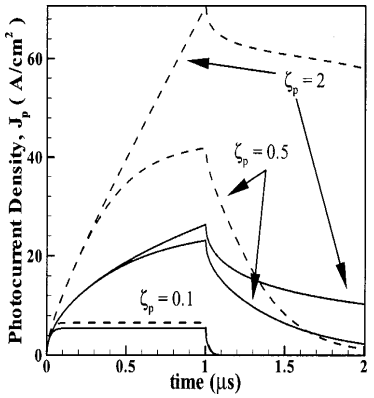

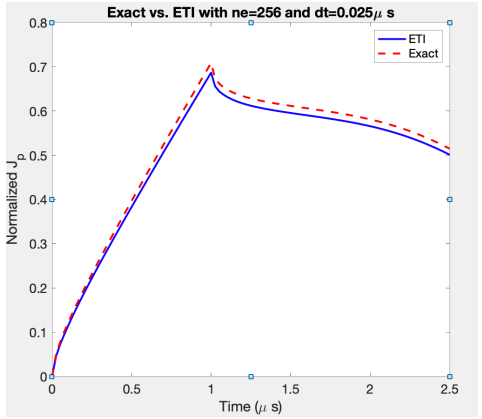

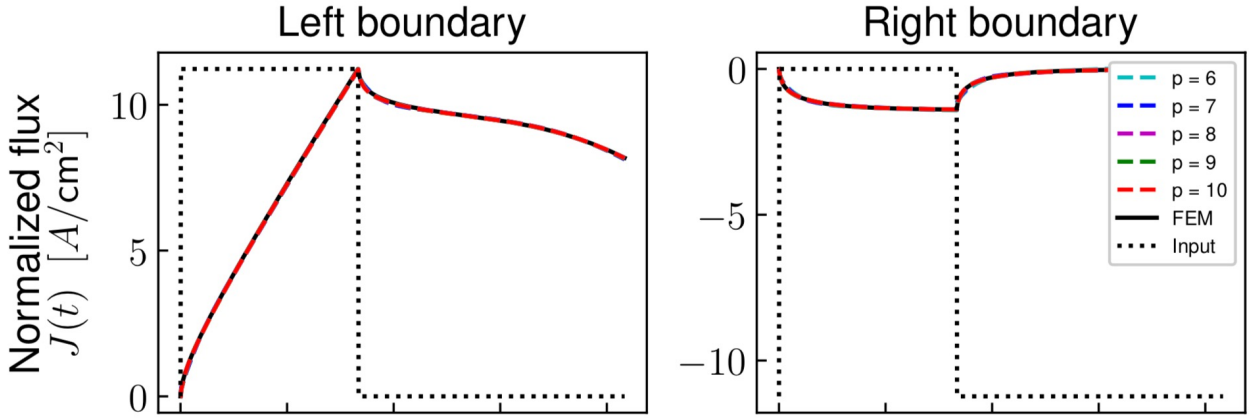

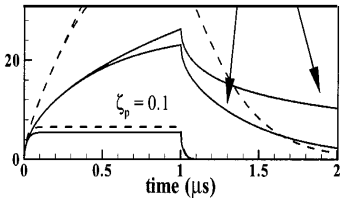

$E = 0$

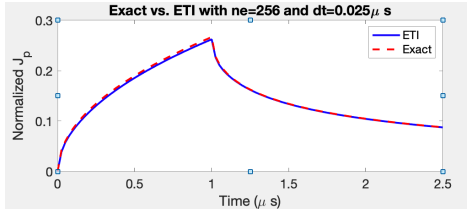

ETI model

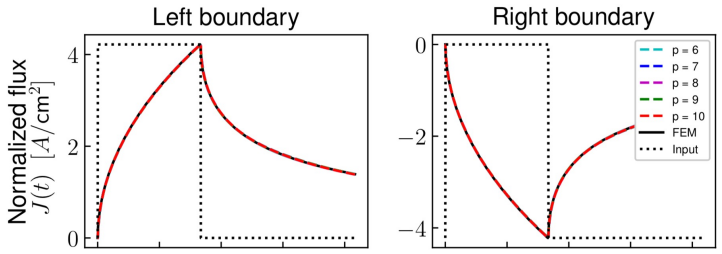

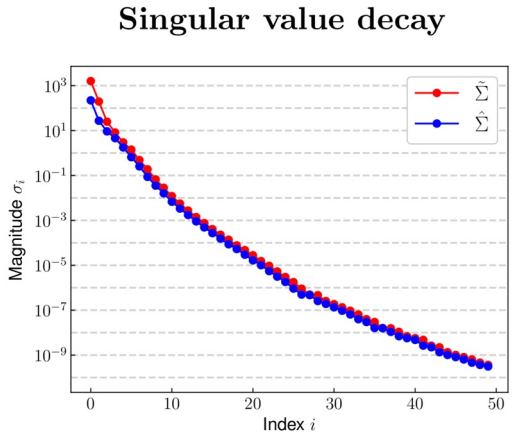

DMD model

Validation: hybrid, ROM-based model for a Zener 5236 diode

- Complex 3D geometry: can be modeled synergistically in TCAD, 2D or 3D
- **Physics-based compact modeling approach** (Xyce Zener photocurrent model for QASPR)
  - Break the device into three 1D PN-junctions: Zener, Guard Ring, Periphery
  - Connect 2 TF photocurrent models to 2 of the PN diodes: **Zener PN** junction and **Guard ring PN** junction
- Our goal is to show that a hybrid, ROM-based model is as good as a state-of-the art analytic Fjeldly (TF) model
  - Simplified setting with a **single, Aggregated PN (APN)** junction (**Zener PN** + **Guard ring PN**)
  - Hybrid photocurrent model connected to the **APN** junction

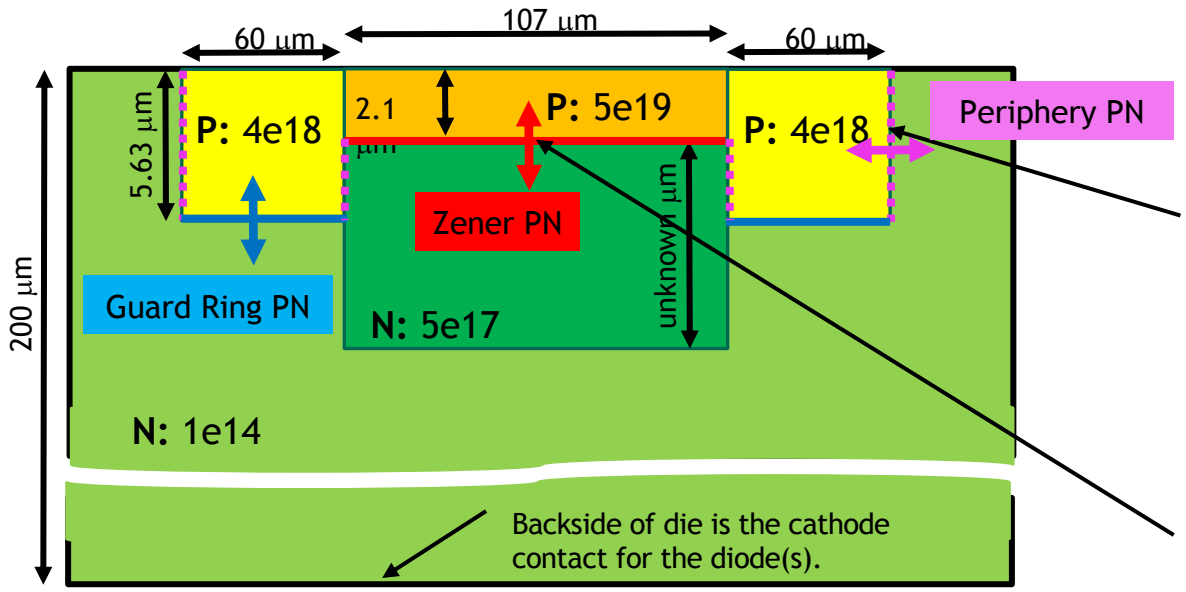

This PN junction intersects the surface of the die but this is unimportant because the breakdown voltage for this diode is greater than the Zener breakdown voltage.

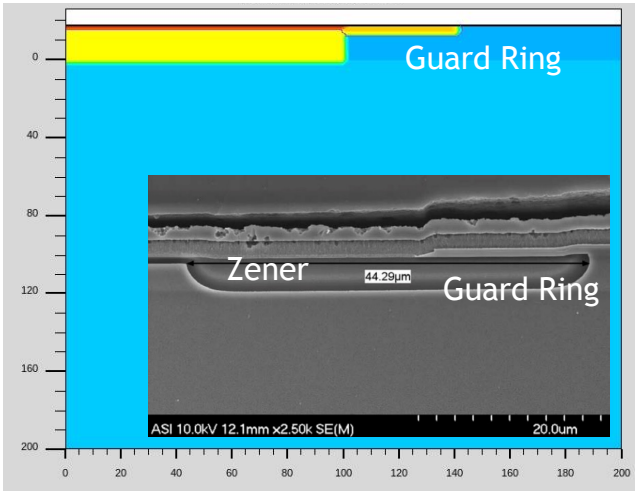

This PN junction is constrained to be at a constant depth and does not terminate at the edge or surface of the die. The breakdown voltage variation is thus reduced.

Photocurrent experimental set up (Little Mountain Test Facility)

Photocurrent data for a batch of Zener Diodes (Z5236) was collected as part of the QASPR project using the Medusa linear accelerator (LINAC) on the Little Mountain Test Facility (LMTF)

Photocurrent measurement schematic

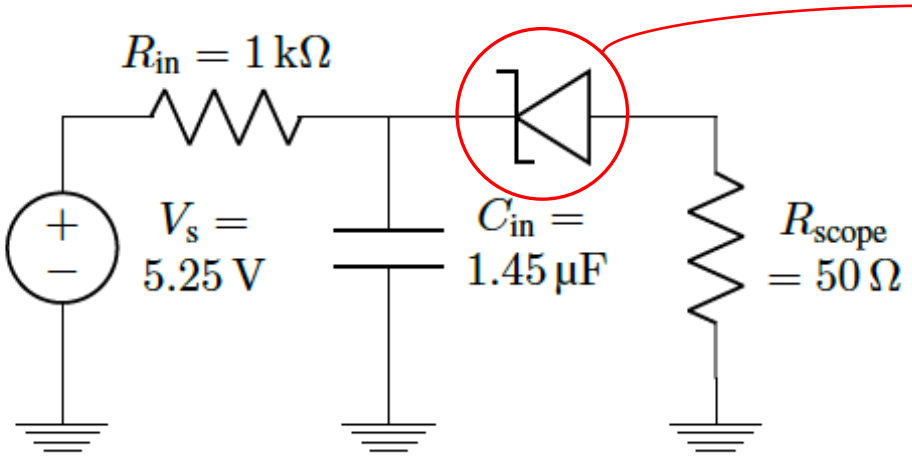

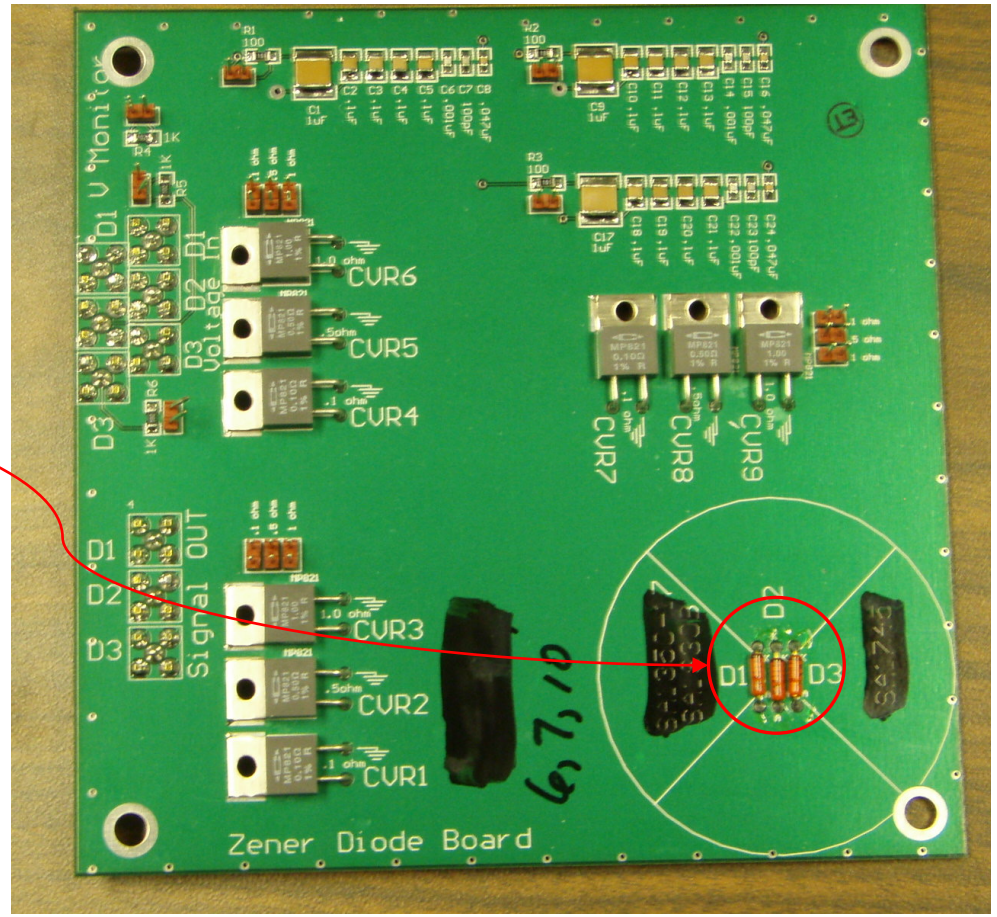

Photocurrent measurements (Little Mountain Test Facility)

Total dose (TD) and pulse width (PW) for the LMTF LINAC Shots

Shot #	How used	TD (rad)	*PW* (s)
435 (Long)	calibration	2250.9	4.95e-6
436 (Long)	prediction	2272.3	4.95e-6
444 (Short)	calibration	53.0	1.05e-7
445 (Short)	prediction	53.5	1.04e-7

$\{I_{k,i}^N\}$ Time series with photocurrent measurement

$\{\gamma_k^N\}$ Time series describing the pulse profile collected by a photo conducting detector (PCD).

Conversion to dose rate (model input)

$$g_k^N = \frac{\gamma_k^N}{\int_{PW} \gamma^N(t)dt} \times TD \times G$$

Transformed PCD signal

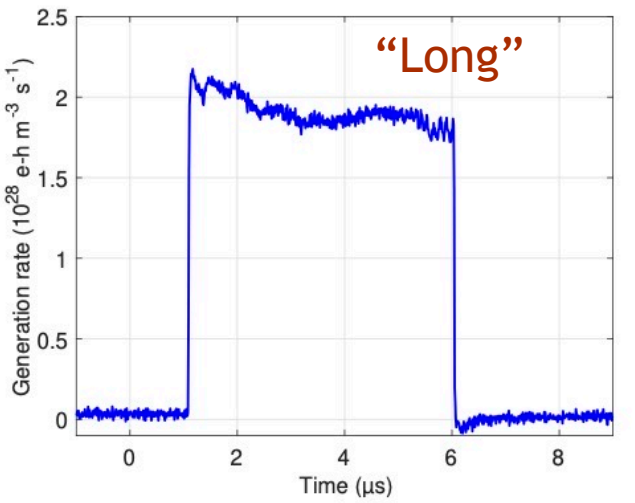

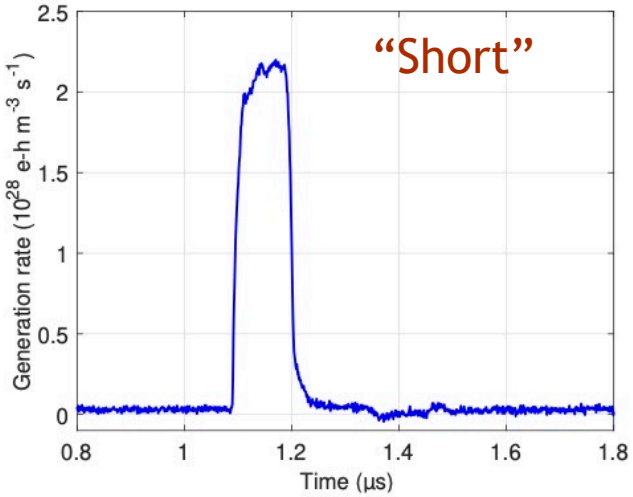

$\{\gamma_k^N\} \rightarrow \{g_k^N\}$

Photocurrent

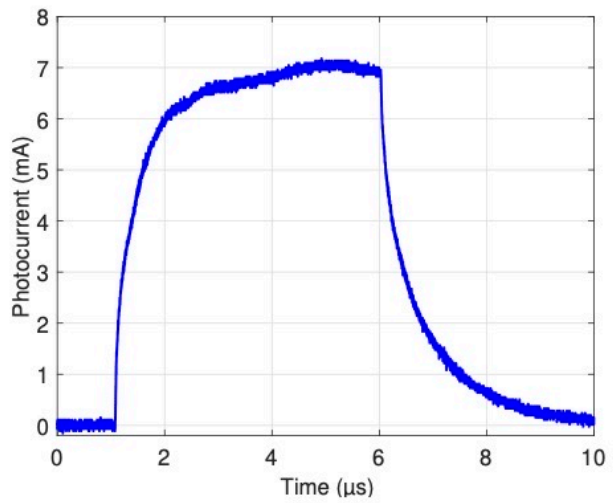

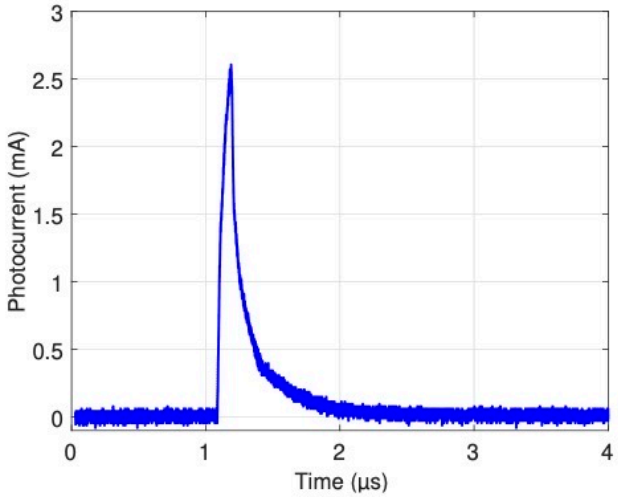

$\{I_{k,i}^N\}$

Model calibration

Both the Fjeldly and the hybrid compact models are calibrated with respect to the same parameter sets:

- udiff*(pdn, ndn, pdp, ndp) — carrier diffusion
- utau*(taun0, tauinfn, taup0, tauinfp) — carrier lifetime
- devarea*area — PN-junction area
- depfrac*wn — N/P region depth

CALIBRATED MODEL PARAMETERS

Model	Hybrid	Fjeldly
D_p^*	7.24×10^{-4}	4.34×10^{-3}
τ_p^*	1.44×10^{-6}	5.99×10^{-7}
τ_p^∞	n/a	1.20×10^{-6}
w_n	1.92×10^{-4}	1.07×10^{-4}
A	6.87×10^{-8}	4.92×10^{-8}
D_n^*	7.24×10^{-4}	1.09×10^{-3}
τ_n^*	7.21×10^{-5}	3.00×10^{-5}
τ_n^∞	n/a	6.00×10^{-5}
w_p	5.63×10^{-6}	5.63×10^{-6}

Error metric for models calibration:

$$M = \left\| I_{train}^{435} - I_{model}^{435} \right\|_{\ell^2}^2 + \left\| I_{train}^{444} - I_{model}^{444} \right\|_{\ell^2}^2$$

- Hybrid model is calibrated at the FOM level (before extracting the ROM)
- The differences in the calibrated values are due to the different model form errors in the hybrid FOM model and the Fjeldly model.
- The calibrated parameters should not be thought of as actual physical values corresponding to the device being tested due to the presence of the model form error.

Calibration accuracy: hybrid vs. Fjeldly

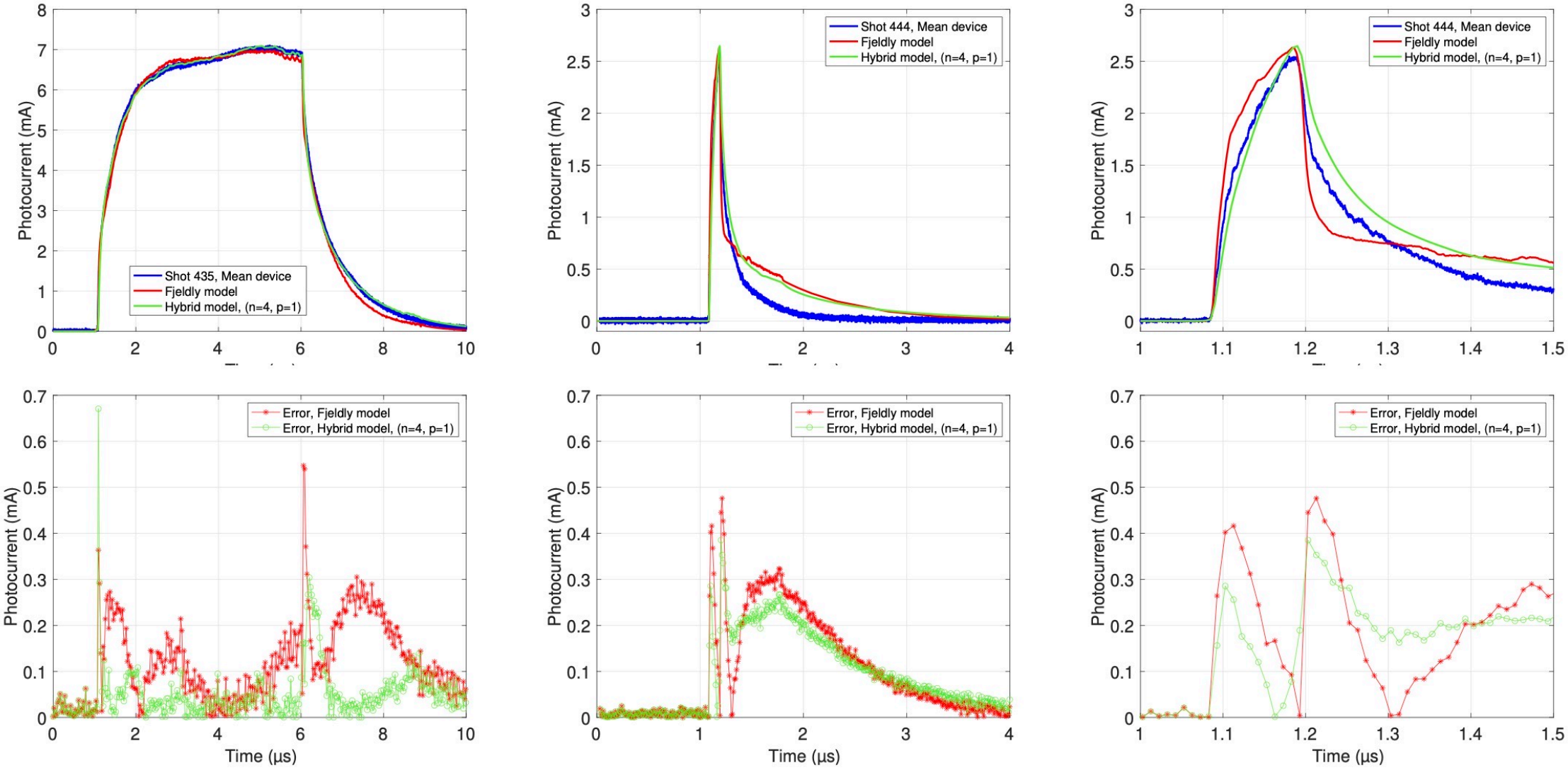

Shots 435 and 444 (calibration data set)

Prediction accuracy: hybrid vs. Fjeldly

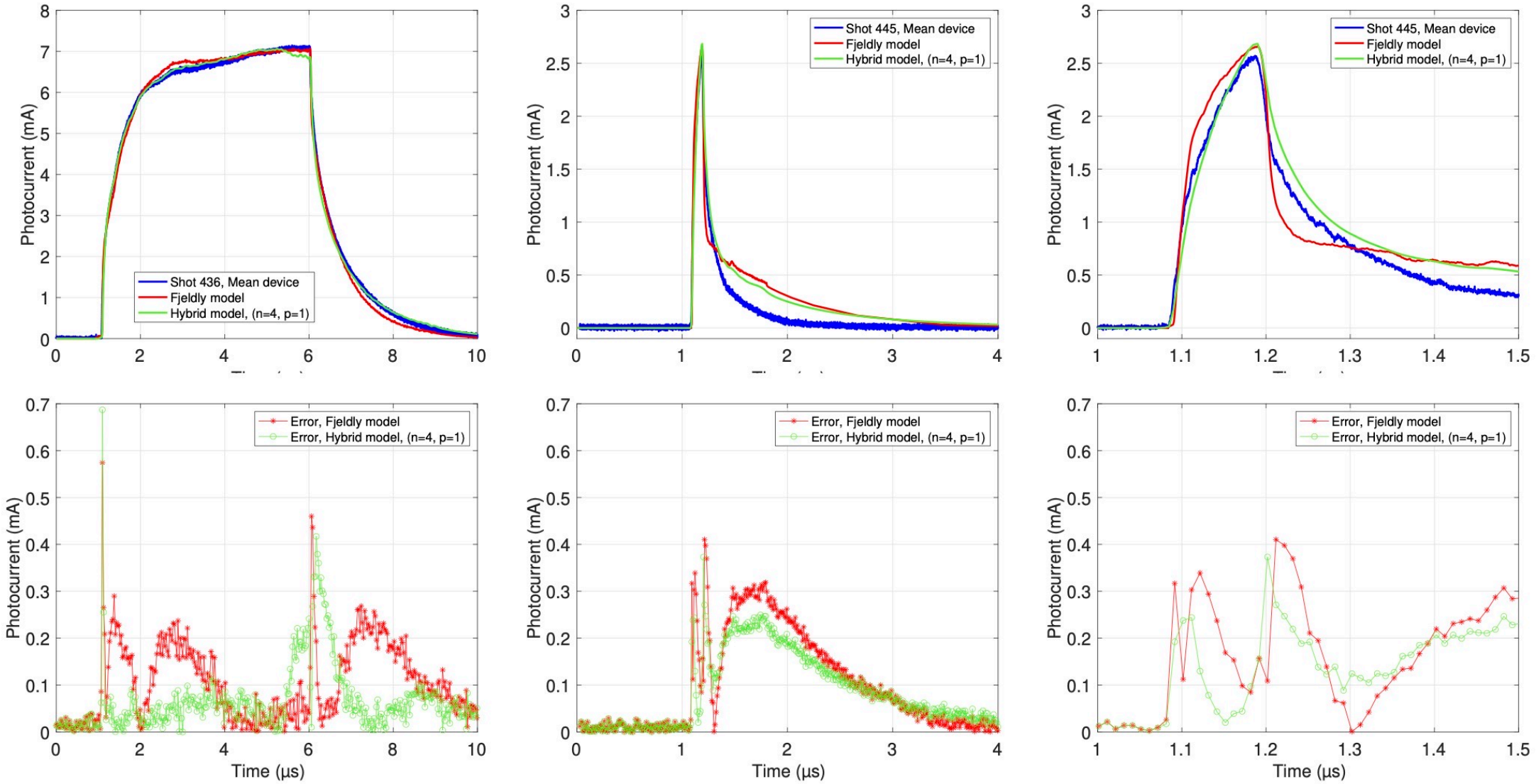

Shots 436 and 445 (prediction data set)

Compression ratio for the reduced order delayed photocurrent model

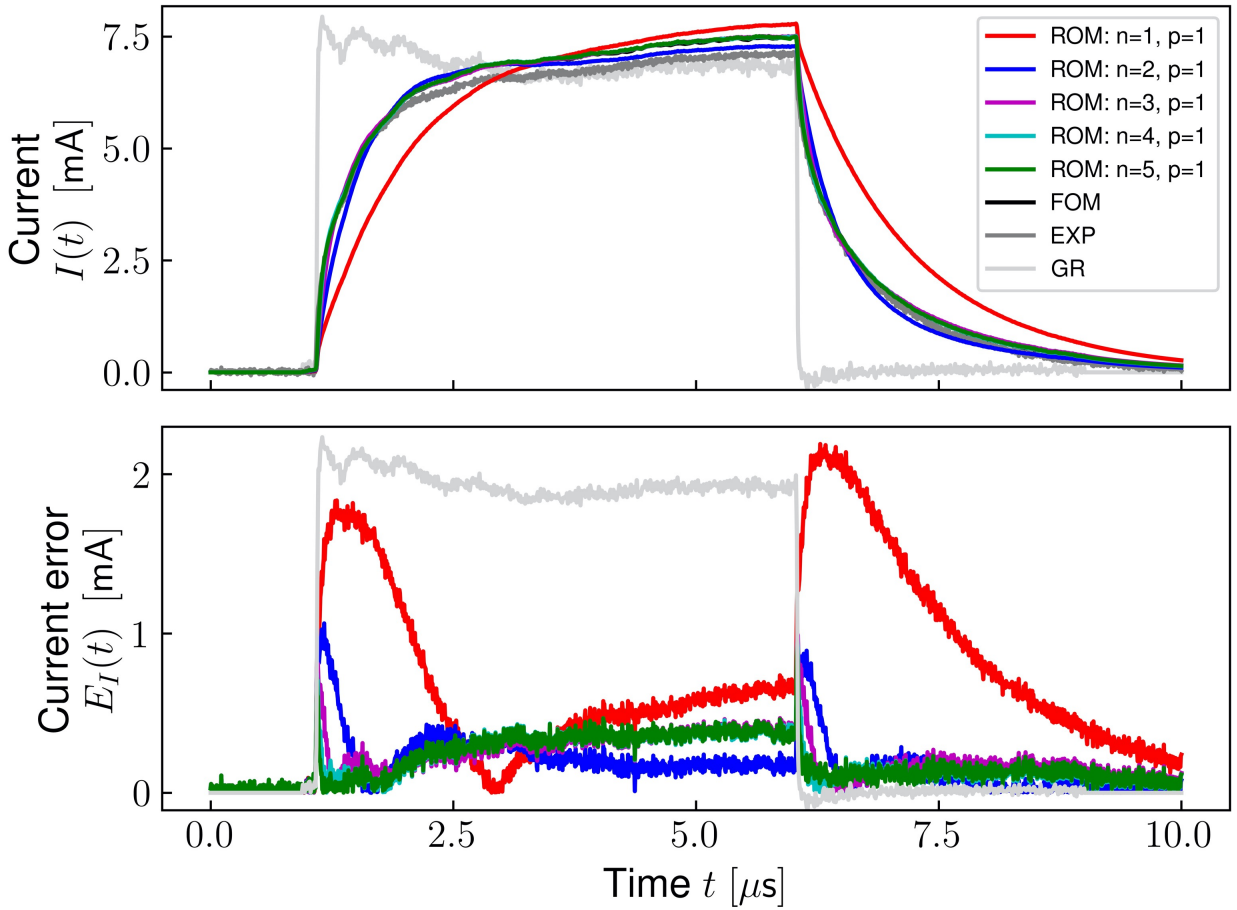

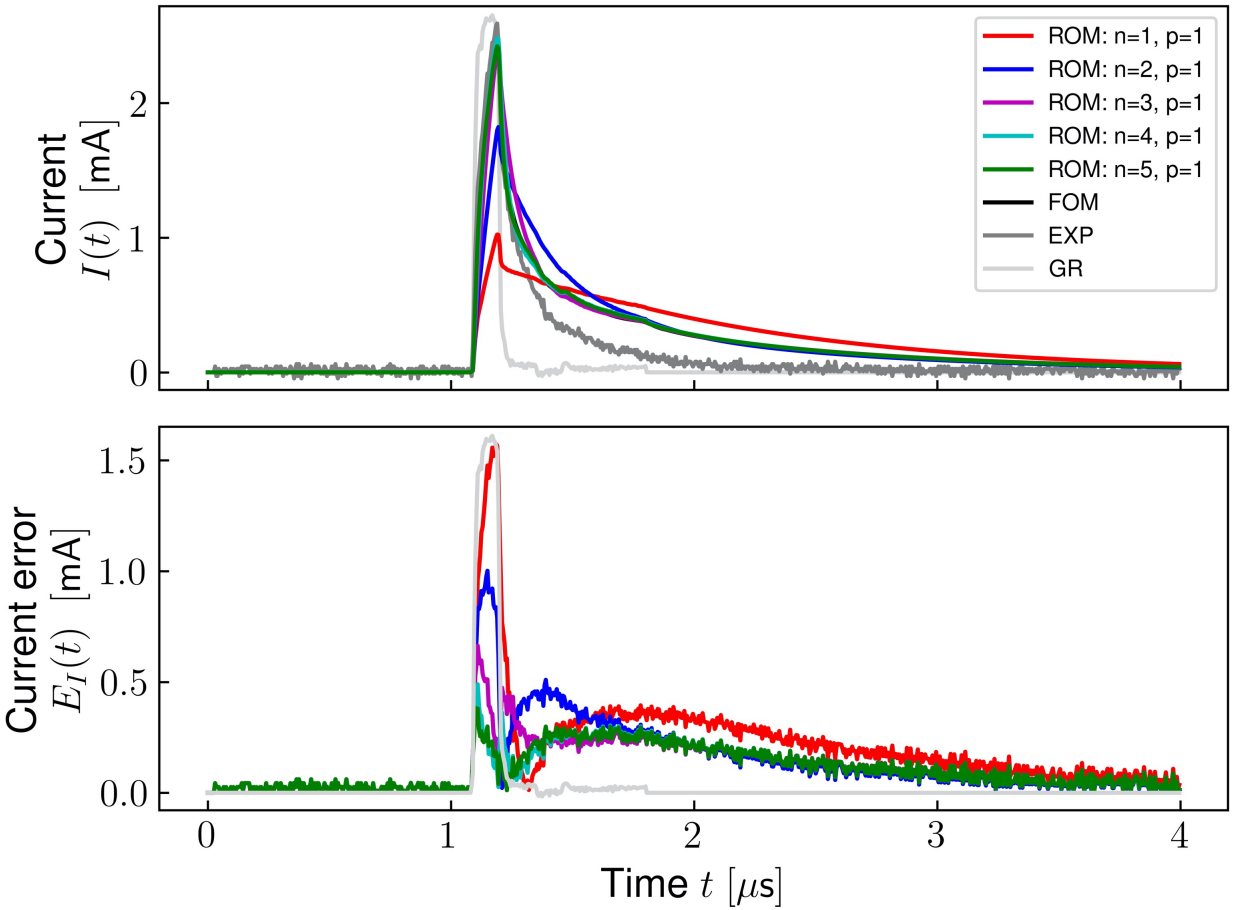

- ADE FOM defined by partitioning Ω_n and Ω_p into 1024 uniform elements: dim(FOM) = 1024*2=2048 ODEs

$ROM_{n=3,p=1}$ - system of 3+1=4 ODEs $\Longrightarrow$ 2048/4=512:1 compression ratio

$ROM_{n=4,p=1}$ - system of 4+1=5 ODEs $\Longrightarrow$ 2048/5~410:1 compression ratio

Remarks

The hybrid ROM-based model was intended to provide a proof-of-principle: **it does not utilize the full power of order reduction** and uses the decomposition into delayed and prompt photocurrents, as well as the **linear ADE** (low injection rate assumption).

This choice was deliberate: we decided to to adopt the **same physics basis** as in the development of traditional compact analytic models for the following two main reasons.

- First, by applying MOR in an "optimal" linear PDE setting where its properties are well-understood, we can assess the potential of the approach without the burden of developing a sophisticated nonlinear reduced order model from scratch.
- Second, by using the same physics basis as in traditional analytic models enables a true apples-to-apples comparison with state of the art analytic models.

Our results indicate moderate, yet noticeable improvements in the predictions of the hybrid model.

Our model also took a much shorter time to develop: the main effort was writing the 1D Finite Element ADE code (<1 week).

Running data-driven models in production circuit simulators

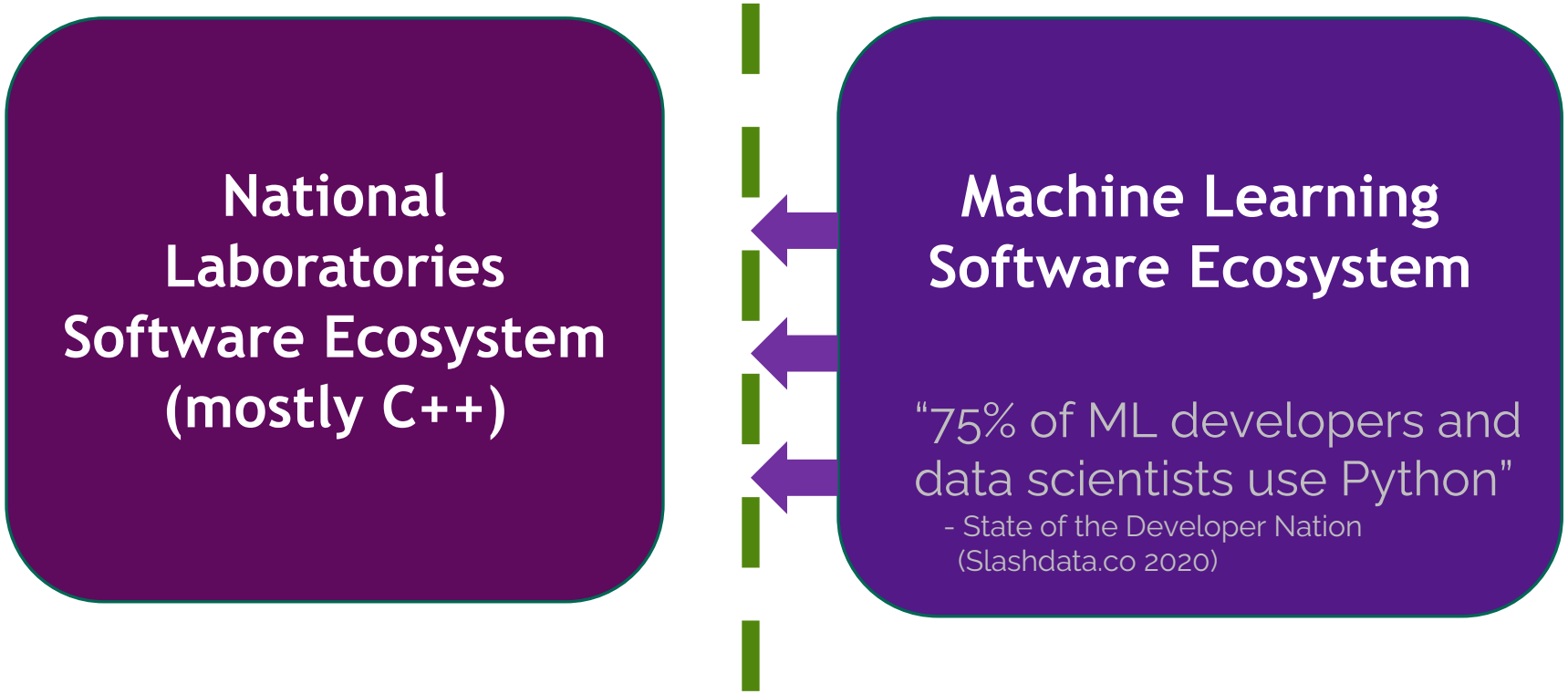

A recent Sandia ASC project (P. Kuberry - PI) aims to enable ML advancements to impact design phases of nuclear deterrence electrical systems via data-driven compact device models.

Running data-driven models in production circuit simulators

Xyce-PyMi is a Xyce Python Model Interpreter for enabling ML advancements in production circuit simulation software.

- P. Kuberry and E. Keiter. An embedded python model interpreter for Xyce™ (Xyce-PyMi). Sandia Report SAND2021-9504, Sandia National Laboratories, 2021.

Example: Operational Amplifier with compact GMLS BJT model vs. Xyce's Gummel-Poon BJT

```
**************
* netlist  for Operational Amplifier
**************
VDD     1    0   DC    2.5
R1 1 4 1e4
R2 1 5 1e4
R3 6 0 5e3
C1 4 0 5e-12
C2 5 0 5e-12
YGENEXT pyQ1 4 7 6
+ SPARAMS={NAME=MODULENAME,DATAFILE
           VALUE=../models/gmls_bjt_2N2222.py,../data/2N2222_alan.01.dat}
RQ1 7 2 50
YGENEXT pyQ2 5 8  6
+ SPARAMS={NAME=MODULENAME,DATAFILE
           VALUE=../models/gmls_bjt_2N2222.py,../data/2N2222_alan.01.dat}
RQ2 8 3 50
Em_plus 2 0 VALUE={1+50e-3*sin(2*pi*10*time)}
Em_minus 3 0 VALUE={1-50e-3*sin(2*pi*10*time)}
```

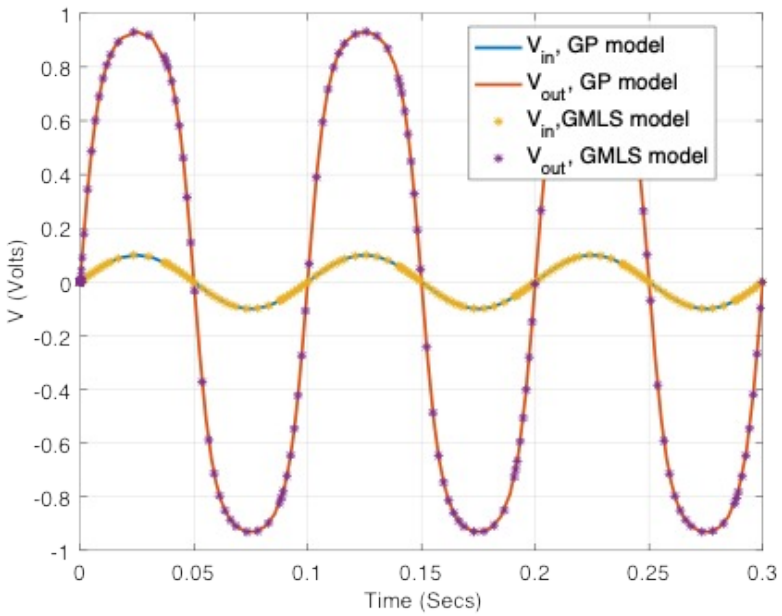

Implementation of the hybrid photocurrent model in Xyce via Xyce PyMi

$$\dot{\boldsymbol{u}}(t) = A\boldsymbol{u}(t) + E(t)N\boldsymbol{u}(t) + Bg(t)$$
$$I(t) = C\boldsymbol{u}(t) + w_D\big(V(t)\big)Dg(t)$$

$$E(t) \propto V_{\mathrm{bi}} - V(t)$$
$$w_D(V(t)) \propto \sqrt{\max(0, V_{\mathrm{bi}} - V(t))}$$

- The ROM parameters are the reduced matrices, which could be stored in a pickle file, .csv, .txt, etc.
- The FOM parameters are calibrated to experiment via TCAD (or ”quasi-TCAD”), then the ROM matrices are extracted automatically.

Translate math to Python code

```python
# Open loop dynamics
def forward(self, t, x, g, V):
    return np.matmul(self.A, x) + 0.5 * (V - self.V_bi) * np.matmul(self.N, x) + self.B * g

# Open loop output
def output(self, t, x, g, V):
    return np.dot(self.C, x) + np.sqrt(np.maximum(0, V - self.V_bi)) * self.D * g

# Closed loop dynamics/output for a given radiation input (descriptor protocol)
def generate_closed_loop(self, input):

    def forward_CL(self, t, x, V):
        return self.forward(t, x, input(t), V)
    self.forward_CL = forward_CL.__get__(self)

    def output_CL(self, t, x, V):
        return self.output(t, x, input(t), V)
    self.output_CL = output_CL.__get__(self)
```

Implementation of the hybrid photocurrent model in Xyce

1. Model form definition (translate math to code):

```
4  class ADE_ROM:
5      def __init__(self, **kwargs):
```

...

```
46      # Open loop dynamics
47      def forward(self, t, x, g, V):
48          return np.matmul(self.A, x) +
49
50      # Open loop output
51      def output(self, t, x, g, V):
52          return np.dot(self.C, x) + np.
```

2. Instantiate model (read in pre-calibrated ROM matrices):

```
1  import numpy as np
2  import pickle
3  import dynamic_models
4
5  # Import matrices
6  with open('Models/ROM_n4p1_matrices.pkl', 'rb') as file:
7      An, Ap, Nn, Np, Bn, Bp, Cn, Cp, D = pickle.load(file)
8
9  # Initialize model
10 ROM = dynamic_models.ADE_ROM(n_dim = 4, p_dim = 1)
11 ROM.An = An
12 ROM.Nn = Nn
13 ROM.Bn = Bn
```

3. Import model instance into Xyce-PyMi custom device definition template:

```
15  class Device(BaseDevice):
16
17      def processPythonParams(self, b_params,
```

...

```
88      def computeXyceVectors(self, fSV, solV, stoV, staV, deviceOpt
89              origFlag, F, Q, B, dFdX, dQdX, dFdXdVp, dQdXdVp,
90              b_params, d_params, i_params, s_params):
```

4. Plug radiation model into netlist ("YGENEXT")

```
1  *
2  * S I M U L A T I O N   D I R E C T I V E S
3  *
4  .TRAN 1.0E-9 14u 0u 0.5E-8
5  .PRINT TRAN I(Rout)
6  *
7  * C I R C U I T   N E T L I S T
8  *
9  Vin           2     0     5.25
10 Rin           2     1     1k
11 Cin           1     0     1.45u
12 Rout          3     0     50
13 Xdiode        3     1     MMSZ5236BT1
14 YGENEXT Iphoto 1    3
15 + SPARAMS={NAME=MODULENAME,MODELFILE,DATAFILE VALUE=RadModels.py,Inst_ADE_ROM.
```

Conclusions

- **Numerical data-driven approaches** for compact photocurrent modeling can circumvent the need for simplifying analytic assumptions and approximations, yielding a “faithful-to-the-physics” model which is fast to develop and easy to implement.
- **Reduced development time: model extraction from underlying data (DMD, ET) or FOM (ROM) is “automated”**
  - Main efforts can be concentrated on the development of FOMs and data acquisition
- **Extraction of compact models** from FOMs has multiple advantages:
  - Compact models and FOMs reference the same physics.
  - Reduces remodeling and produces more generalizable, more credible compact models.
  - These models require less-per-instance calibration:
    - Reduced calibration data gathering, formatting, and storage burdens.
    - Accelerated end-to-end ModSym process.
- **Follow-up work:**
  - Projection-based ROM utilizing polynomialization has been developed for the nonlinear ADE showing excellent results
  - Use simple physics-based descriptions (which can achieve high compression ratios) and augment the model with perturbations (e.g., neural nets) to achieve a close fit to experimental measurements.